21st Australasian Fluid Mechanics Conference
Adelaide, Australia
10-13 December 2018

Recovery of a turbulent boundary layer following a rough-to-smooth step-change in the wall condition

M. L. Mogeng[1], C. M. de Silva[1], R. Baidya[1], A. Rouhi[1], D. Chung[1], I. Marusic[1], N. Hutchins[1]

[1]Department of Mechanical Engineering
University of Melbourne, Victoria 3010, Australia

Abstract

This paper examines the recovery of a turbulent boundary layer that has undergone a sudden streamwise transition from a rough-walled to a smooth-walled surface. Despite studies over the past few decades these flows are yet to be fully understood. In particular, these attempts have been hampered by reliability issues in determining the local wall-shear stress after the transition [1], where many existing tools for measuring the wall-shear stress fail due to non-equilibrium, non-canonical conditions. Here, we utilise a collection of experimental databases at $Re_\tau \approx 3500$ with direct measures of the wall-shear stress to understand the recovery to equilibrium conditions to the new surface. Our results reveal that for distances less than $0.5\delta_0$ (where δ_0 is the boundary layer thickness at the roughness transition) downstream of the rough-to-smooth transition the wall-shear stress for the current configuration exhibits variation in the spanwise direction. Further, the mean velocity in the buffer region and beyond appears to take several boundary layer thicknesses downstream of the roughness change to recover to the equilibrium state. Through a spectral analysis of the energetic modes of the flow, we also observe that the recovery of small-scale streamwise velocity fluctuations in the near-wall region is achieved over shorter downstream distances compared to the larger scales.

Introduction

Surface roughness with heterogeneity is present in wall-bounded turbulent flows in a variety of conditions. For example, the patchiness of biofouling on the hull of a ship or the changes in the surface roughness conditions that occur at the interface between forest and grasslands. For this study we consider the simplified geometry of a rough-to-smooth transition occurring in the streamwise direction. This configuration is best described with reference to figure 1, where upstream of the transition, an equilibrium rough wall boundary layer has developed over the rough fetch. Following the transition, the new smooth wall condition initially modifies the near-wall region, which then gradually propagates towards the interior of the flow with increasing distance downstream of the transition. The layer that separates the modified near-wall region (which 'sees' the new smooth wall condition) from the unaffected oncoming flow, further away from the wall (which 'remembers' the rough-wall condition) is generally referred to as the internal boundary layer (IBL) with a thickness denoted by δ_i [4].

Although the streamwise rough-to-smooth heterogeneity has been studied extensively over the past few decades [1, 5, 10], to date, the recovery to equilibrium conditions of the new surface following such a transition is far from understood. For example, determining the local wall-shear stress τ_w after the transition (and subsequently the friction velocity U_τ) have been hampered by reliability issues [1], where many existing tools for measuring the recovering wall-shear stress fail due to non-equilibrium, non-canonical conditions (causing problems for Clauser fits, Preston tubes and the like). In addition, in turbulent boundary layers without roughness heterogeneity, it has been well-established that the turbulence fluctuations over a rough surface are more energetic compared to its smooth-wall counterpart, while the near-wall cycle, on the other hand, is suppressed [11]. However, how these over-energised motions in the outer part adapt to the new wall condition, and how the near-wall cycles re-establish downstream of the rough-to-smooth change under the influence of the over-energised outer motions is yet to be fully understood.

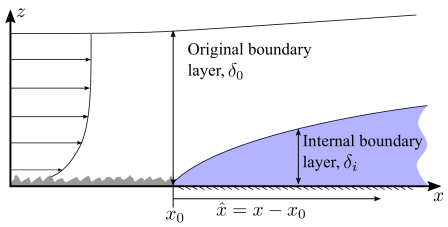

Figure 1: Schematic of a turbulent boundary layer flow over a rough-to-smooth change in surface condition. Flow is from left to right and $\hat{x} = x - x_0$ represents the fetch measured from the rough-to-smooth transition which occurs at $x = x_0$.

We aim to bridge the gap and redress some previous issues by directly measuring the recovering skin-friction coefficient C_f using Oil Film Interferometry (OFI). The recovery of the turbulence fluctuation and the near-wall cycle is studied through the examination of the pre-multiplied energy spectra.

Throughout this paper, the coordinate system x, y and z refer to the streamwise, spanwise and wall-normal directions, respectively. Corresponding velocity fluctuation components are represented by u, v and w. The rough-to-smooth transition occurs at $x = x_0$, and we use the ordinate $\hat{x} = x - x_0$ for the fetch on the smooth wall downstream of the transition. The boundary layer thickness at the rough-to-smooth transition is denoted as δ_0. Capital letters indicate spanwise- and/or time-averaged quantities and the superscript + refers to inner normalisation with the local velocity scale as $U_\tau(\hat{x})$. For example, we use $l^+ = lU_\tau/\nu$ for length and $u^+ = u/U_\tau$ for velocity, where ν is the kinematic viscosity of the fluid.

Experimental databases

The current experimental data are acquired in an open-return boundary layer wind tunnel facility in the Walter Basset Aerodynamics Laboratory at the University of Melbourne. Further details can be found in [9].

The arrangement of the experimental campaign consisting of hotwire boundary layer traverses and OFI measurements are depicted in figure 2. In the present work, the first 3.7 m of the tunnel surface is covered by P16 grit sandpaper, while the remaining streamwise length is a smooth surface. Details of the roughness parameters are obtained by scanning a 60 mm × 60 mm

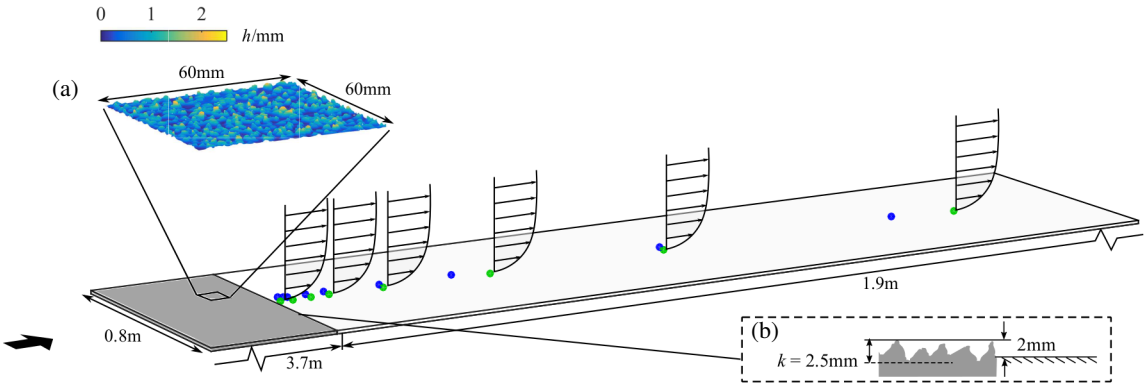

Figure 2: Overview of the experimental setup in the open-return boundary layer wind tunnel facility at $Re_\tau \approx 3500$. The ● symbols correspond to the locations of the hotwire wall-normal profiles, and the ● symbols are where OFI measurements are performed. Note that a small spanwise shift is employed for the symbols in the schematic for clarity, which is not the case in the actual experiments. The colour contours in the inset (a) illustrates the topography of the rough-walled surface (P16 sandpaper, indicated by a shaded region in the main figure), and (b) is a schematic showing the relative height of the roughness and the smooth surface.

section of the sandpaper using an in-house laser scanner. The roughness peak height k (maximum height difference between the crest and trough of the roughness) is approximately 2.5 mm, which is equivalent to 3% of the boundary layer thickness $\delta_0 = 88.5$ mm at the surface transition ($k/\delta_0 \approx 0.03$), and the maximum roughness crest is about 2 mm above the smooth wall (see figure 2b). For more details on the measurement, the readers are referred to [2].

Hotwire Anemometry

A conventional single-wire hotwire probe of 2.5 µm diameter is operated by an in-house Melbourne University Constant Temperature Anemometer (MUCTA). Boundary layer profiles are measured at $\hat{x}$ = 10, 30, 60, 90, 180, 360, 660 and 1190 mm (● symbols in figure 2), corresponding to $\hat{x}/\delta_0$ = 0.1, 0.3, 0.7, 1.0, 2.0, 4.1, 7.5 and 13.4, respectively. The occasional mismatch in the streamwise location of hotwire and OFI measurements is a consequence of limited optical access.

Oil Film Interferometry

The wall-shear stress, τ_w, is measured using OFI [3], which is one of the few methods available for a direct measurement at the surface. A line of silicon oil with a nominal viscosity of 100 cSt is placed on a clear glass surface, perpendicular to the main flow direction, and illuminated by a monochromatic light source from a sodium lamp. The resulting interference pattern is captured using a Nikon D800 DSLR camera. The FOV of the OFI measurements is calibrated with a calibration grid featuring a 2.5 mm dot spacing, providing a conversion from image to real space. The measurement is repeated twice at each streamwise location.

For each OFI measurement, 100 images are captured separated by a time interval of 5 s. The image sequences are then processed using an FFT based algorithm [8] to extract the fringe spacing of the interferograms. Thereafter, a linear trend is fitted to the extracted fringe spacing of the interferograms versus time to evaluate the wall-shear stress, τ_w. Note that this process is performed independently for every line of pixels in y for the entire spanwise extent of the oil film, which is between 10–20 mm for each repeated measurement. Regions contaminated by dust are removed during processing. The resulting spanwise profile of the skin-friction coefficient is denoted as $\widetilde{C}_f(\hat{x},y) = \tau_w(\hat{x},y)/\frac{1}{2}\rho U_\infty^2$ (U_∞ is the freestream velocity), and $C_f(\hat{x})$ is the spanwise average of $\widetilde{C}_f(\hat{x},y)$.

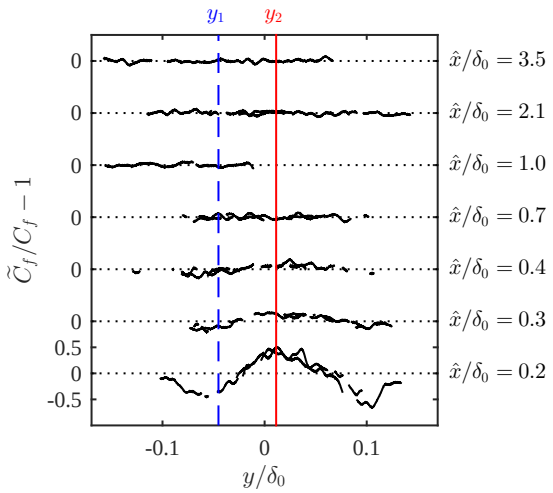

Figure 3: Relative spanwise variation of the skin-friction coefficient, $\widetilde{C}_f/C_f - 1$. Regions contaminated by dust are not shown in the figure. $y = 0$ is approximately the centreline of the tunnel, and the vertical dashed blue line and solid red line indicate regions of low skin-friction at $y_1/\delta_0 = -0.045$ and high skin-friction at $y_2/\delta_0 = 0.011$, respectively.

Results and Discussion

Spanwise Variation of the Skin-friction Coefficient

A measure of the spanwise variation of $\widetilde{C}_f(\hat{x},y)$ from the OFI measurements is shown in figure 3. At $\hat{x}/\delta_0 = 0.2$, $\widetilde{C}_f$ varies by more than 50% about its mean value. Typical low and high skin-friction regions are identified at $y_1/\delta_0 = -0.045$ (blue dashed line) and $y_2/\delta_0 = 0.011$ (red solid line), respectively. The variation of $\widetilde{C}_f$ appears to be influenced by the distribution of the roughness elements immediately prior to the rough-to-smooth transition. We also note this variation remains in the same spanwise location further downstream, while the amplitude of the variation diminishes rapidly within a short fetch. More specifically, $\widetilde{C}_f$ is nominally constant for all y locations measured beyond $\hat{x}/\delta_0 = 0.5$, which is equivalent to $\hat{x}/k = 20$ in this study.

The recovery of the spanwise averaged C_f as a function of $\hat{x}$ is shown in figure 4. The overall trend of C_f exhibits an undershoot immediately downstream of the rough-to-smooth step

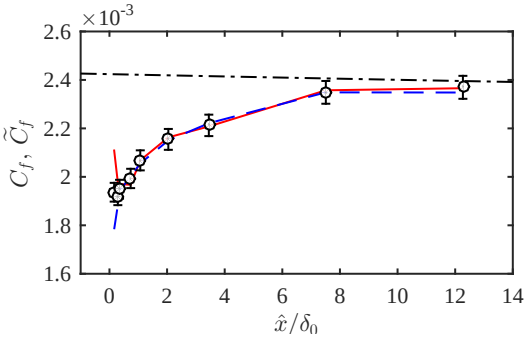

Figure 4: The spanwise averaged skin-friction coefficient $C_f(\hat{x})$ measured by OFI (∘ symbols). The dashed blue and solid red lines show $\widetilde{C}_f$ obtained at fixed spanwise locations, $y_1/\delta_0 = -0.045$ and $y_2/\delta_0 = 0.011$, respectively (vertical lines in figure 3). The dot-dashed line corresponds to C_f of a canonical smooth-wall boundary layer predicted by integrating the von Kármán momentum integral equation [7]. A total uncertainty of ±2% in $\widetilde{C}_f$ contributed by the oil viscosity (±0.5%) and the pitot tube (±1%) is shown by the error bars.

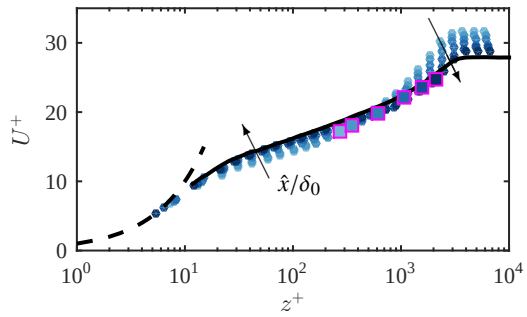

Figure 5: Viscous scaled mean streamwise velocity profiles U^+. The shading of the symbols indicate downstream fetch from the step change, where from lightest to darkest $\hat{x}/\delta_0 = 0.7, 1.0, 2.0, 4.0, 7.5, 13.4$. The dashed black line corresponds to the linear relationship $z^+ = U^+$ of the viscous sublayer, and the solid black line corresponds to a reference smooth-wall dataset obtained at Re_τ matched with the most downstream profile. Square symbols show the location of the IBL for each velocity profile following the approach of [10].

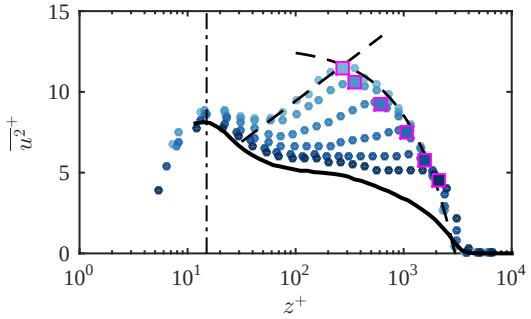

Figure 6: Viscous scaled streamwise turbulence intensity $\overline{u^2}^+$. Symbols and corresponding colours are the same as figure 5. The solid black line corresponds to the reference smooth-wall dataset as in figure 5, the dot-dashed line indicates $z^+ = 15$, and the dashed lines are an example of the curve fit at $\hat{x}/\delta_0 = 0.7$ to locate δ_i.

change, and a gradual recovery towards the value of an equilibrium smooth-wall boundary layer as shown by the dot-dashed line calculated using the boundary layer evolution model [7]. The blue and red lines are the $\widetilde{C}_f$ obtained along a streamwise line at fixed spanwise locations y_1 and y_2 (as shown in figure 3), respectively. These results highlight that immediately downstream of the roughness transition, a strong variation in the recovery of the skin-friction coefficient may occur depending on the chosen spanwise location, thus measurements at a single spanwise location in this region must be interpreted with caution.

Recovery of the Mean Flow

We utilise the hotwire data to further investigate the recovery of the mean flow statistics. The mean streamwise velocity profiles are shown in figure 5, with the black dashed line indicating the law of the wall and the solid line a reference smooth-wall dataset obtained at a Re_τ matched with the most downstream profile. Here, the friction velocity $U_\tau(\hat{x})$ is calculated from the spanwise averaged skin-friction coefficient C_f, interpolated at a streamwise location $\hat{x}$. We note that the first two hotwire profiles at $\hat{x}/\delta_0 = 0.1$ and 0.3 are not shown here since our measure of $U_\tau(\hat{x})$ might be compromised by the spanwise variation of the viscous scale (see figure 3). In any case, the main focus here is on the general effect of the rough-to-smooth change rather than the localised influence of individual roughness elements. The results exhibit good collapse at $z^+ \lesssim 10$, however, there is a general lack of agreement in the buffer region and beyond, despite the fact that this region is well below the IBL thickness (to be detailed in the following subsection). This confirms that the flow within the IBL is not in equilibrium with the local wall condition [1]. Moreover, these results confirm that methods relying on the mean velocity information in buffer region and above (e.g. Preston tube, Clauser chart method) are unlikely to provide a reliable wall-shear stress measurement for several δ_0 downstream of the roughness change [2]. This, in turn, explains some of the scatter reported in the literature for the wall-shear stress after a rough-to-smooth change.

Recovery of the Streamwise Turbulence Fluctuation

Figure 6 shows hotwire profiles of the viscous-scaled streamwise turbulence intensity $\overline{u^2}^+$, at various locations downstream of the roughness transition. These are compared against a profile taken from a fully smooth surface at a Re_τ matched with the most downstream profile. We note that the attenuation of the inner-peak due to a finite sensor length [6] is not corrected for these profiles, but is expected to be comparable between all cases since the wire length is kept constant in viscous units ($l^+ \approx 20$). For the present case, the IBL thickness δ_i, is defined as the 'knee-point' in the streamwise turbulence intensity profile following [10], and is estimated by finding the intersection of two curve fits above and below the point where a sudden change in $\overline{u^2}^+$ occurs (dashed lines in figure 6). The results show that the turbulence intensity within the IBL shows a monotonic decay towards the equilibrium smooth-wall reference, while little change is observed beyond the IBL. We note, at the furthest downstream location ($\hat{x}/\delta_0 = 13.4$), the measured $\overline{u^2}^+$ has still not recovered to an equilibrium state to the new wall-conditions and the IBL thickness δ_i is only approximately half of the local boundary layer thickness δ_{99}. It is worth noting that although the location of the inner-peak seems to be approximately fixed at $z^+ \approx 15$ (dot-dashed line in figure 6) as in an equilibrium smooth-walled boundary layer, the intensity is higher and appears to decrease monotonically with the downstream fetch.

Streamwise Energy Spectrum

To further investigate the contribution to the excess energy in the inner-peak, one dimensional pre-multiplied spectra of the

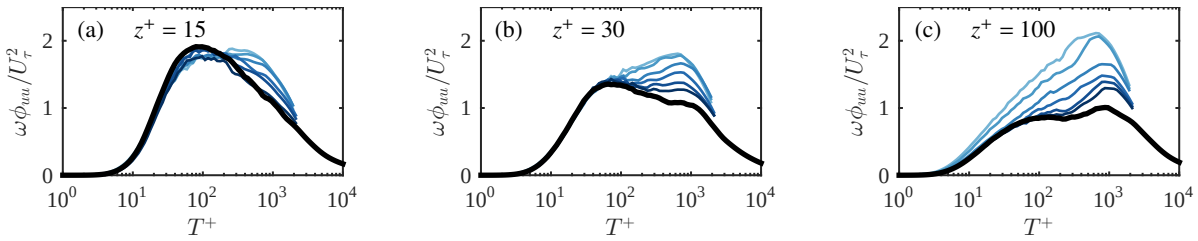

Figure 7: Viscous scaled pre-multiplied energy spectra of the streamwise velocity component $\omega\phi_{uu}/U_\tau^2$ at (a) $z^+ = 15$, (b) $z^+ = 30$ and (c) $z^+ = 100$. The colour scheme is the same as in figure 5, and the black curve represents a smooth-wall reference at matched Re_τ.

streamwise velocity component $\omega\phi_{uu}/U_\tau^2$ are calculated and presented in figure 7, where $\omega = 2\pi f$ (in rad s^{-1}) is the angular frequency, and ϕ_{uu} is the energy spectrum of the streamwise velocity fluctuations. Since the flow is heterogeneous in x, we refrain from converting the spectrum from a temporal to spatial domain using Taylor's hypothesis. Further, the spectrograms presented are computed from hotwire time sequences, in segments of 3×10^3 samples (equivalent to 0.1s, or $17\delta_0/U_\infty$) with an overlap of 50%, to guarantee that the small- and intermediate- scales are well converged.

Figure 7a shows the spectrum at the inner-peak location ($z^+ = 15$). The peak in the spectrum in the smooth-wall reference occurs at $T^+ = 2\pi/\omega^+ \approx 90$, equivalent to $\lambda_x^+ \approx 1000$. Further, excess energy (relative to the smooth wall reference) appears to reside at time scales larger than $T^+ = 200$, and diminishes with distance downstream from the transition, while the small-scale energy appears to exhibit good agreement with the reference within the experimental uncertainty. Similar trends are also observed at $z^+ = 30$ (see figure 7b), while further away from the wall a distinct deviation from the reference is observed at $z^+ = 100$ for $\hat{x}/\delta_0 = 0.7$ and 1.0 even at the smaller-scales present in the flow. It should be noted that $\delta_i^+ \approx 270$ at $\hat{x}/\delta_0 = 0.7$, thus this deviation may be related to the proximity of the IBL to the reference location in this case. Nevertheless, for positions closer to the wall and sufficiently lower than the IBL, the small energetic scales following the rough-to-smooth transition seem to recover rapidly to a canonical smooth wall behaviour. It is likely that the over energised large-scale motions are presumably an artefact from the rough surface, representing the superimposed footprint of large-scales that are located beyond the IBL.

Conclusion

This work presents an experimental study of a turbulent boundary layer with streamwise heterogeneity in surface roughness. Our results reveal that the wall-shear stress within approximately $0.5\delta_0$ (or approximately 20 roughness heights) downstream of the rough-to-smooth transition suffers from variations in the spanwise direction for the present configuration. Furthermore, we demonstrate that wall-shear stress measuring techniques that rely on the mean velocity in the buffer region and above are not applicable immediately downstream of the roughness change, and a fetch of several δ_0 over the smooth surface is required for the mean flow in the buffer region to reach an equilibrium state to the new wall conditions. Further, an over-energised inner-peak is observed in the streamwise turbulence intensity profile. This behaviour is explained by examining the energy spectrum, which reveals a high-energy 'footprint' of the large-scale fluctuations, while the small-scales are observed to adapt to the new smooth wall condition within one δ_0 downstream of the rough-to-smooth transition.

Acknowledgement

The finacial support of the Australian Research Council is gratefully acknowledged.

References

[1] Antonia, R. A. and Luxton, R. E., The response of a turbulent boundary layer to a step change in surface roughness. Part 2. rough-to-smooth, *J. Fluid Mech.*, **53**, 1972, 737–757.

[2] de Silva, C. M., Mogeng, M. L., Baidya, R., Rouhi, A., Chung, D., Marusic, I. and Hutchins, N., Estimating the wall-shear stress after a rough-to-smooth step-change in turbulent boundary layers using near-wall PIV/PTV experiments, in *Proc. 19th Intl. Symp. Applic. Laser Tech. Fluid Mech., Lisbon, Portugal*, 2018.

[3] Fernholz, H. H., Janke, G., Schober, M., Wagner, P. M. and Warnack, D., New developments and applications of skin-friction measuring techniques, *Meas. Sci. Tech.*, **7**, 1996, 1396–1409.

[4] Garratt, J. R., The internal boundary layer - A review, *Boundary-Layer Meteorol.*, **50**, 1990, 171–203.

[5] Hanson, R. E. and Ganapathisubramani, B., Development of turbulent boundary layers past a step change in wall roughness, *J Fluid Mech.*, **795**, 2016, 494–523.

[6] Hutchins, N., Nickels, T. B., Marusic, I. and Chong, M. S., Hot-wire spatial resolution issues in wall-bounded turbulence, *J Fluid Mech.*, **635**, 2009, 103–136.

[7] Monty, J. P., Dogan, E., Hanson, R., Scardino, A. J., Ganapathisubramani, B. and Hutchins, N., An assessment of the ship drag penalty arising from light calcareous tubeworm fouling, *Biofouling*, **32**, 2016, 451–464.

[8] Ng, H. C. H., Marusic, I., Monty, J. P., Hutchins, N. and Chong, M. S., Oil film interferometry in high Reynolds number turbulent boundary layers, in *Proc. 16th Australian Fluid Mech. Conf., Gold Coast, Australia*, 2007.

[9] Nugroho, B., Hutchins, N. and Monty, J. P., Large-scale spanwise periodicity in a turbulent boundary layer induced by highly ordered and directional surface roughness, *Int. J. Heat Fluid Flow*, **41**, 2013, 90–102.

[10] Saito, N. and Pullin, D. I., Large eddy simulation of smooth–rough–smooth transitions in turbulent channel flows, *Int. J. Heat Mass Trans.*, **78**, 2014, 707–720.

[11] Squire, D. T., Morrill-Winter, C., Hutchins, N., Schultz, M. P., Klewicki, J. C. and Marusic, I., Comparison of turbulent boundary layers over smooth and rough surfaces up to high Reynolds numbers, *J. Fluid Mech.*, **795**, 2016, 210–240.